

Lack of collisional hydrodynamics in a harmonically trapped one-dimensional Bose gas

Caroline Mauron,¹ Karen V. Kheruntsyan,^{1,*} and Giulia De Rosi^{2,†}

¹*School of Mathematics and Physics, University of Queensland, Brisbane, Queensland 4072, Australia*

²*Departament de Física, Universitat Politècnica de Catalunya, Campus Nord B4-B5, 08034 Barcelona, Spain*

(Dated: August 12, 2025)

Using the theory of generalized hydrodynamics, we study the dipole compression collective oscillations of a harmonically trapped one-dimensional Bose gas in the crossover from weak to strong repulsive interactions. In the uniform limit, the system is described by the integrable Lieb-Liniger model, while the presence of the trap breaks integrability. In contrast to previous predictions based on the classical hydrodynamic variational ansatz—which yields a single-frequency dipole compression mode—we observe a beating signal comprising two frequencies across all regimes of the gas. Furthermore, we find that the higher frequency crosses over from the low-temperature *phononic* hydrodynamic regime to the *collisionless* limit as the temperature increases—without saturating at the previously predicted value characteristic of the high-temperature *collisional* hydrodynamic regime. This crossover occurs around the so-called hole-induced anomaly temperature, above which the quasiparticle picture of excitations no longer applies. This explains the absence of the collisional hydrodynamic regime and resolves a long-standing open question about its validity at high temperatures in systems where integrability is nearly broken by weak confinement. Our findings reveal intricate connections between excitations, thermodynamics, correlations, dynamics, and interparticle collisions, and may prove relevant to other atomic, nuclear, solid-state, electronic, and spin systems that exhibit similar anomalies or thermal second-order phase transitions.

Introduction—Many-body systems are ubiquitous across a broad range of disciplines, including chemistry, materials science, condensed matter, and nuclear, molecular, and atomic physics [1, 2]. By tuning the interparticle interaction strength and temperature, one can explore diverse phases of matter and regimes, in which the system properties change at macroscopic (e.g., thermodynamics, collective dynamics) and microscopic (e.g., excitations, correlations, and collisions) levels. Remarkably, the large-scale motion of a variety of generic (non-integrable) systems is often well described by classical hydrodynamics (HD) [3], which relies on few conservation laws, such as for particle number, momentum, and energy, together with rapid local thermalization in the collisional regime. HD applies to nuclear matter [4, 5], solids [6], magnetic materials [7], liquid helium [8], and ultracold atomic gases [9–12]. Integrable systems, by contrast, admit exact solutions and an infinite set of conserved quantities [13, 14], which preclude thermalization [15–20], thereby challenging the validity of collisional HD.

At low temperatures T , classical HD equations describe the dynamics of various systems, provided that the low-momentum (long-wavelength) quasiparticle excitations are phononic in nature, as in the one-dimensional (1D) Bose gas [21–23]. In a harmonic trap, phonons manifest as collective normal modes with discrete frequencies, involving slow variations of the system’s macroscopic properties rather than fast microscopic particle motion. HD is valid for any superfluid at $T = 0$ K [11, 22], including Bose and Fermi gases and strongly interacting helium [12]. In 1D, any thermal phase transition, such as superfluidity and Bose-Einstein condensation (BEC), is forbidden in the thermodynamic limit [24–26], and the HD equations remain applicable at finite T without re-

quiring the description of coupled superfluid and normal components (Landau’s two-fluid theory) [12, 26]. The same occurs in an ideal Fermi gas [11, 27], where superfluidity is absent due to the lack of interactions.

At high T , even for $T > T_c$ [11, 28] (where T_c is the critical temperature of the phase transition), classical HD may still apply, provided that rapid and frequent interparticle collisions drive the system toward local thermal equilibrium. The high- T collisional HD regime is expected to hold when $\omega \ll \Gamma$ [9, 12], where ω is the collective mode frequency and Γ the collision rate. However, as temperature increases further, the density decay induced by the harmonic trap makes collisions rare and any gas inevitably ends up in the collisionless (CL) regime (see Appendix A), captured by the classical ideal gas model.

In this Letter, we address whether a harmonically trapped 1D Bose gas enters a collisional HD regime. While the uniform system is integrable, this question is particularly relevant under weak confinement, which slightly breaks integrability and thus hinders fast thermalization. To this end, we use dipole-compressional (DC) oscillations [11, 29–31] as a probe, since their frequencies at high temperatures differ between the collisional HD regime [30] and the CL regime [11, 31], as shown in Table I. This behavior contrasts with that of the lowest breathing mode—extensively studied experimentally and theoretically [11, 22, 30–41]—which has the same frequency in both regimes. The 1D Bose gas can be realized in ultracold atom chips, optical lattices and tube traps [42–45], making it an ideal platform to study DC modes, which have been measured in Fermi gases [29].

To investigate the DC oscillations, we employ the theory of generalized hydrodynamics (GHD) [46, 47], which keeps track of the infinitely many conserved local quanti-

Table I. Hydrodynamic vs. collisionless frequencies of dipole compression modes in a 1D Bose gas for weak and strong interactions [11, 31]. ω_x is the axial harmonic trap frequency.

	Hydrodynamic		Collisionless
	$T = 0$ K	high T	
Weak interactions	$\sqrt{6}\omega_x$	$\sqrt{7}\omega_x$	$3\omega_x, 1\omega_x$
Strong interactions	$3\omega_x$	$\sqrt{7}\omega_x$	$3\omega_x, 1\omega_x$

ties in integrable systems and thus extends beyond classical HD [48–56]. Unlike classical HD—which accounts for only a few macroscopic conserved properties—GHD is capable of capturing also the collisionless regime. Even when integrability is weakly broken, GHD remains applicable within the local density approximation (LDA) [49, 52, 56, 57]. Our GHD simulations thus serve as a numerical experiment, and provide evidence for the absence of a high- T collisional HD regime. Instead, they reveal a thermal crossover from phononic HD to CL behavior around the hole-induced anomaly temperature T_A [58]. We therefore propose that $T < T_A$ serves as a sufficient and universal criterion for the applicability of classical HD, restricting it only to the phononic HD regime.

The hole-induced anomaly was recently identified in a uniform 1D Bose gas at arbitrary interaction strength. It refers to a thermal feature appearing in several thermodynamic properties as a function of temperature [58, 59], such as a peak in the specific heat at $T \approx T_A$. More generally, an anomaly arises in any 1D gas exhibiting phonons [58]. Similar anomalies occur in atomic, solid-state, electronic, and spin systems as a result of a second-order phase transition (where $T_c = T_A$) [26, 60, 61], or due to a thermal population in the excitation spectrum [58, 62, 63]. At $T \approx T_A$, the low- T quasiparticle description breaks down [58, 64] and, for $T \gtrsim T_A$, thermal fluctuations prevail over quantum correlations, strongly affecting the tails of the momentum distribution [58, 59]. This Letter sheds light on the impact of the hole-induced anomaly on collective dynamics and collisional effects, thereby completing a universal framework that links microscopic and macroscopic phenomena in 1D Bose gases.

Model—The Hamiltonian for the harmonically trapped 1D Bose gas is given by [57, 65]

$$H = -\frac{\hbar^2}{2m} \sum_{i=1}^N \frac{\partial^2}{\partial x_i^2} + g_{1D} \sum_{i>j}^N \delta(x_i - x_j) + \sum_{i=1}^N V(x_i), \quad (1)$$

where m is the particle mass, N is the total number of bosons, and $V(x) = m\omega_x^2 x^2/2$ is the axial harmonic trap with frequency ω_x . The interaction strength is $g_{1D} \simeq 2\hbar\omega_\perp a$ [66] for repulsive ($a > 0$) contact interactions, with ω_\perp the transverse harmonic confinement frequency and a the three-dimensional (3D) s -wave scattering length.

In the absence of the trap, $V(x) = 0$, the density $n = N/L$ (where L is the length of the system) is con-

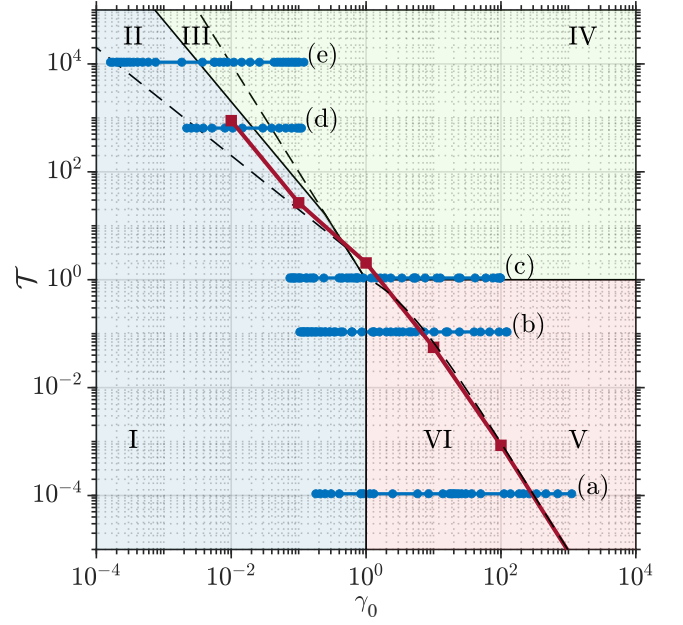


Figure 1. Diagram of regimes of the harmonically trapped 1D Bose gas in terms of the interaction strength γ_0 and temperature T (2). Regimes are [73]: I. Bogoliubov (quantum), $T/2 \ll \gamma_0^{-1}, \gamma_0 \ll 1$; II. Bogoliubov (thermal), $2\gamma_0^{-1} \ll T \ll 2\gamma_0^{-3/2}$; III. Nearly ideal Bose gas (degenerate), $2\gamma_0^{-3/2} \ll T \ll \gamma_0^{-2}$; IV. Nearly ideal Bose gas (non-degenerate), $T \gg \max\{1, \gamma_0^{-2}\}$; V. Strong interactions (high T), $\pi^2/(\gamma_0 + 2)^2 \ll T \ll 1, \gamma_0 \gg 1$; VI. Strong interactions (low T), $T \ll \pi^2/(\gamma_0 + 2)^2, \gamma_0 \gg 1$. Red thick solid line denotes the anomaly temperature T_A vs. γ_0 , where the red square markers represent the values of T_A estimated from the position of the peak in the specific heat [58]. Datasets (a)-(e) (blue points), are used for the study of dipole compression modes in regimes I-VI, and are calculated at fixed T .

stant in x and the Hamiltonian reduces to the integrable Lieb-Liniger model [21, 67]. This framework is exactly solvable via the Bethe ansatz [68, 69] for its $T=0$ ground state and the spectrum of excitations, as well as for finite- T thermodynamic properties using Yang-Yang’s thermal Bethe ansatz [70–72]. When $V(x) \neq 0$, the system becomes non-integrable, and the spatial density profile $n(x)$ determines $N = \int dx n(x)$. Under weak confinement, the gas is approximately uniform locally, allowing the use of the LDA [57], where $n(x)$ follows from the local chemical potential $\mu[n(x)] = \mu_0 - V(x)$ with $\mu_0 = \mu(x=0)$.

The system (1) is conveniently characterized by the dimensionless interaction strength and temperature [57]:

$$\gamma_0 = \frac{mg_{1D}}{\hbar^2 n_0}, \quad \mathcal{T} = \frac{T/T_d}{\gamma_0^2} = \frac{2\hbar^2 k_B T}{mg_{1D}^2}, \quad (2)$$

where $T_d = \hbar^2 n_0^2/(2mk_B)$ is the quantum degeneracy temperature at the central density $n_0 = n(x=0)$, whereas \mathcal{T} is the global temperature, independent of density and x .

Figure 1 shows the diagram of different regimes of the 1D Bose gas [57, 58, 65, 72–75] in the γ_0 - \mathcal{T} parameter

space. The points on the horizontal lines (a)–(e) depict the datasets of this work. Progressing to the right along a given line corresponds to increasing values of the interaction strength at the trap center γ_0 , associated with decreasing densities n_0 . Datasets (a)–(e) span all relevant physical regimes, including the weakly interacting quasicondensate regions I and II, described by Bogoliubov theory [76]; the degenerate (III) and non-degenerate (IV) regimes, both approaching the ideal ($\gamma_0 \rightarrow 0$) Bose gas; and the strongly interacting high- T (V) and low- T (VI) behaviors, which for $\gamma_0 \rightarrow \infty$ recover the Tonks-Girardeau limit, where the thermodynamics is the same as that of an ideal Fermi gas [77]. Figure 1 also reports the dimensionless hole-induced anomaly temperature T_A as a function of γ_0 [58], which intersects datasets (a)–(d). The values of T_A (red squares) are obtained from the peak of the specific heat in the uniform system with the same γ_0 as in the trap. For dataset (e), which lies in the very weakly interacting regime ($\gamma_0 < 10^{-1}$), the peak is barely discernible, so no T_A is shown.

For fixed γ_0 and T , a third parameter is needed to fully describe a confined gas—typically the trap frequency ω_x , which sets the atom number N , or vice versa. In Appendix B, we report N as a function of γ_0 for datasets (a)–(e) at fixed ω_x , along with the parameters of our calculations of the DC frequencies. We also discuss the experimental conditions required to access regimes I–VI.

Dipole Compression Modes — We initialize the system, Eq. (1), in a finite- T equilibrium state using the exact thermal Bethe ansatz within the LDA [57]. To excite DC oscillations, we apply at time $t = 0$ a quench to the harmonic trap potential $V(x) \rightarrow V(x) - \lambda(x^3/3 - x\langle x^2 \rangle)$ [31], where λ is a small perturbation strength and $\langle x^2 \rangle$ is the average evaluated with the initial (pre-quench) equilibrium density profile $n(x)$ [78] (Appendix C).

To characterize the ensuing DC modes, we compute the time evolution of the perturbed density $n(x, t)$ using the equations of GHD [46, 47], which are implemented with the *iFluid* package [79], as in Ref. [56]. GHD was developed only in 2016 to describe the collective dynamics of integrable and nearly-integrable systems out of thermal equilibrium. GHD provides accurate predictions at length scales much larger than the average interparticle distance, where the gas can be modelled as a continuous fluid in local thermal equilibrium. GHD evolves the quasiparticle distribution according to simple transport equations and has been benchmarked and validated in numerous theoretical and experimental studies [48–53, 55].

Once $n(x, t)$ is computed over a sufficiently long time period, we extract the frequencies of the DC oscillations from the Fourier spectrum of the skewness of $n(x, t)$ (see Appendix D). The resulting spectra typically exhibit two dominant peaks, indicating a beating of two DC frequencies; the positions of the peaks correspond to the said frequencies, ω_1 and $\omega_2 > \omega_1$. We also characterize their relative excitation strengths $K_{1,2}$ via the peak heights

$h_{1,2}$, using $K_1 = h_1^2/(h_1^2 + h_2^2)$ and $K_2 = 1 - K_1$ [41].

Figure 2 summarizes our GHD results for the DC frequencies $\omega_{1,2}$ and their $K_{1,2}$ as functions of the interaction strength γ_0 , Eq. (2). The different panels correspond to datasets (a)–(e) (see also Table II, Appendix B). For comparison, we also present the predictions of the classical HD variational ansatz (CHDVA) [30] as red triangles. For all datasets (a)–(e), increasing γ_0 is equivalent to raising the temperature, as the system is driven into the two high- T regimes IV and V, see Fig. 1. In panels (a)–(d), vertical red lines mark the values of γ_0 at the anomaly temperature, $\gamma_0^A \equiv \gamma_0(T = T_A)$, where T_A intersects (a)–(d) in Fig. 1.

For $\gamma_0 > \gamma_0^A$, equivalent to temperatures $T > T_A$, the GHD simulations confirm the existence of the collisionless regime, identified by the beating of two frequency components, $\omega_1 \simeq 1\omega_x$ and $\omega_2 \simeq 3\omega_x$ [31]. However, unlike Ref. [31], which predicted equal excitation strengths for these frequencies (Table I), we find that the low-energy component ω_1 dominates ω_2 as $K_1 > K_2$. This discrepancy is explained by the hole-induced anomaly, arising from the thermal occupation of states located below the lowest hole branch in the spectrum [58]. The excitation of these low-energy states is confirmed by the behavior of the dynamic structure factor (DSF) at $T > T_A$ [58].

For $\gamma_0 < \gamma_0^A$ ($T < T_A$), we instead observe that ω_2 dominates over ω_1 , as $K_2 > K_1$. This is again consistent with the DSF at $T < T_A$, which reveals the excitation of high-energy states located above the hole branch of the spectrum [58]. Our GHD results for the ω_2 component agree with the CHDVA predictions, and both recover the HD analytical limit $\omega_2 = \sqrt{6}\omega_x$ of the Bogoliubov regime I at $\gamma_0 \ll \gamma_0^A$ ($T \ll T_A$), thereby confirming the existence of the phononic HD at low temperatures (see Table I).

We therefore conclude that the anomaly temperature T_A defines a new energy scale governing the HD-CL transition. Since T_A depends on γ_0 [58], the single universal condition $T < T_A(\gamma_0)$ is sufficient to determine the phononic HD regime for any interaction strength. This contrasts with the corresponding two independent conditions in γ_0 and T of Ref. [30]. Physically, the relevance of the anomaly mechanism for the validity of the HD regime is confirmed by the breakdown of the effective low-temperature quasiparticle picture at $T \approx T_A$, as evidenced by the DSF [58]. Notably, a similar trend is observed in systems of higher spatial dimensionality undergoing superfluid or BEC phase transitions: when crossing the critical temperature T_c , the DSF reveals a transition from well-defined collective quasiparticle excitations at $T < T_c$ to a broad thermal response for $T > T_c$.

Next, the CHDVA findings from Ref. [30] disagree with our GHD results. Qualitatively, CHDVA predicts a single frequency across all regimes, whereas GHD reveals a beating pattern involving two distinct frequencies, whose excitation strengths $K_{1,2}$ vary with γ_0 . Quantitatively, at $\gamma_0 \gg \gamma_0^A$ ($T \gg T_A$), the CHDVA frequency asymp-

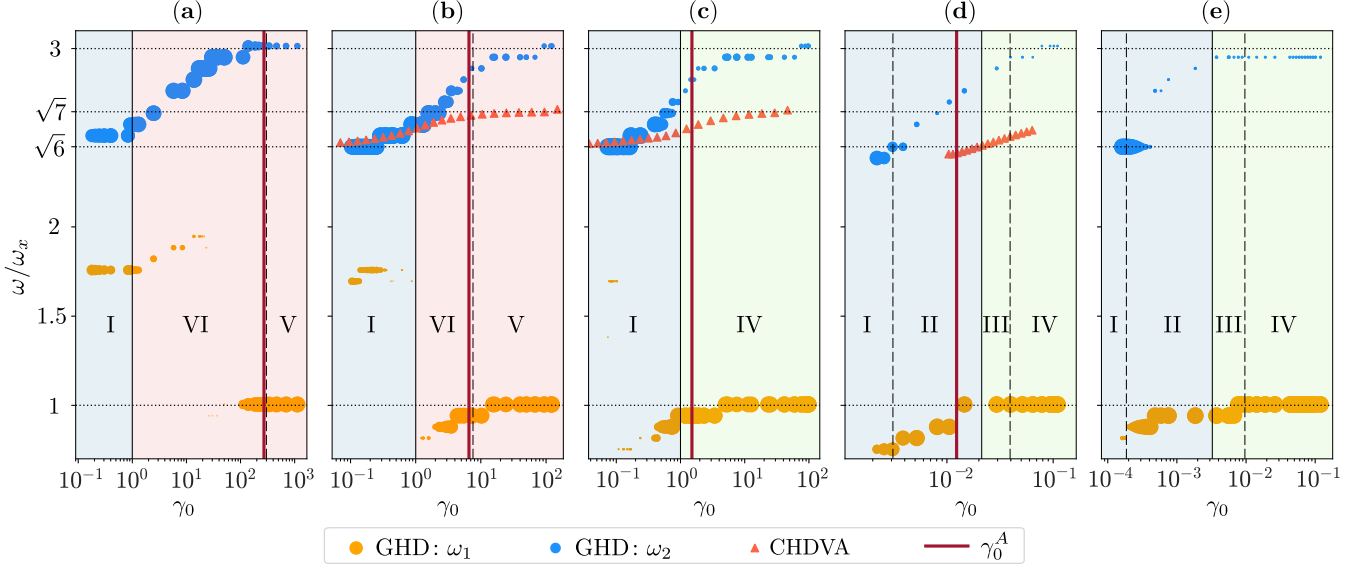


Figure 2. Frequencies ω/ω_x of the dipole compression modes vs. the interaction strength γ_0 , Eq. (2), for datasets (a)-(e), shown in the panels, which span the regimes I-VI of the 1D Bose gas of Fig. 1. Additional parameter values of our simulations are listed in Appendix B, Table II. The two dominant frequency components, ω_1 (lower) and ω_2 (higher), are extracted from generalized hydrodynamics (GHD) calculations of the Fourier transform of the skewness (Appendix D). The sizes of the respective yellow and blue markers are proportional to the excitation strengths K_1 and K_2 . Red triangles indicate the predictions from Ref. [30] obtained using the classical hydrodynamic variational ansatz (CHDVA). Dotted horizontal lines at $\omega/\omega_x = \{1, \sqrt{6}, \sqrt{7}, 3\}$ mark the analytic limits of Table I. Vertical solid red lines denote the interaction strength at the anomaly temperature $\gamma_0^A \equiv \gamma_0(T = T_A)$, whose values are: (a) $\gamma_0^A = 2.86 \times 10^2$; (b) 6.57; (c) 1.51; (d) 1.23×10^{-2} .

totically approaches the value $\sqrt{7}\omega_x$, corresponding to the prediction for the high-temperature collisional HD regime in Table I. However, our GHD results show that ω_2 transitions from $\sqrt{6}\omega_x$ through $\sqrt{7}\omega_x$ at intermediate γ_0 —without saturating there—and continues to increase until it reaches the CL limit $3\omega_x$ at very large γ_0 . These observations confirm: (i) the absence of the high- T collisional HD regime in a 1D Bose gas, in contrast with previous theoretical predictions [11, 30, 31]; and (ii) the failure of classical hydrodynamic approaches—including CHDVA—to capture the CL behavior, which instead requires the GHD framework.

Finally, in panels (a)–(c), for $\gamma_0 \ll \gamma_0^A$ ($T \ll T_A$), the GHD frequency ω_1 recovers the phononic HD limits for the lowest breathing (LB) mode, with values $\omega_1 = \sqrt{3}\omega_x$ and $\omega_1 = 2\omega_x$, corresponding to the low-temperature regimes I and VI, respectively [11, 30, 31, 36, 40]. This result is remarkable, as our GHD simulations were performed without applying the specific LB-mode perturbation to the trap, $V(x) \rightarrow V(x) - \lambda(x^2 - \langle x^2 \rangle)$ [31]. This suggests that, in the present DC oscillation, the LB mode emerges naturally at very low T , with ω_1 being coupled to ω_2 . Moreover, in all panels at $\gamma_0 \sim \gamma_0^A$, we even see $\omega_1 < \omega_x$ —a mode at low excitation energy, which also appears in the DSF at $T \sim T_A$ [58]. As γ_0 (or the temperature) increases, the LB oscillation gradually weakens and eventually vanishes in favour of the component $\omega_1 \simeq 1\omega_x$ corresponding to the center-of-mass (dipole) mode.

Conclusions—We presented a systematic numerical study of the thermal crossover of dipole compression mode frequencies in a harmonically trapped 1D Bose gas with arbitrary interaction strength. Our results: (i) demonstrate the absence of a high- T collisional hydrodynamic regime; (ii) reveal a beating of two DC frequencies, whose excitation strengths thermally evolve consistently with the dynamic structure factor and the hole-induced anomaly [58]; (iii) show that the higher frequency crosses from low- T phononic HD behavior to a high- T collisionless regime around the anomaly temperature $T \approx T_A$; and (iv) indicate that the lower frequency corresponds to the excitation of the LB mode which transitions into the center-of-mass oscillation with temperature.

The new universal temperature scale for the HD-CL transition, set by the anomaly, may explain the mismatch between measurements and HD theory of LB frequencies in the crossover from regime II (thermal quasicondensate), through III (degenerate nearly ideal Bose gas), and into IV (non-degenerate nearly ideal Bose gas) [36].

An anomaly-induced suppression of collisional HD is expected in other 1D systems, such as the super Tonks-Girardeau gas [34, 80], dipolar [81, 82] and Rydberg [83] ensembles, ^3He gas [84], liquid ^4He [85, 86], liquids in mixtures [87, 88], and spin chains [47]. It is intriguing to explore systems where the anomaly manifests as a superfluid or BEC transition, such as in Fermi [89] and Bose [90] atomic gases, and in nuclear matter in stars [91–93].

Acknowledgments—The authors thank H. Hu and X.-J. Liu for kindly sharing the CHDVA data from Ref. [30] shown in Fig. 2 for comparison purposes. C.M. is grateful for the computational support of I. Mortimer and the Core Computing Facility “Getafix” of the School of Mathematics and Physics at the University of Queensland. K.V.K. acknowledges support by the Australian Research Council Discovery Project Grant No. DP240101033. G.D.R. received funding from the Universitat Politècnica de Catalunya (ALECTORS2024, R-02673) and the grant IJC2020-043542-I funded by MCIN/AEI/10.13039/501100011033 and by “European Union NextGenerationEU/PRTR”. G.D.R. also acknowledges support by the Spanish Ministerio de Ciencia e Innovación (MCIN/AEI/10.13039/501100011033, Grant PID2023-147469NB-C21), and by the Generalitat de Catalunya (Grant 2021 SGR 01411).

Author Contributions—G. D. R. devised the initial concepts and the theoretical framework. C.M. performed the GHD numerical simulations under the supervision of K.V.K. All authors contributed to the analysis, interpretation and visualization of the results. G.D.R. and K.V.K. jointly wrote the manuscript.

* karen.kheruntsyan@uq.edu.au

† giulia.de.rosi@upc.edu

- [1] I. Bloch, J. Dalibard, and W. Zwerger, Many-body physics with ultracold gases, *Rev. Mod. Phys.* **80**, 885 (2008).
- [2] P. Coleman, *Introduction to Many-Body Physics* (Cambridge University Press, 2015).
- [3] L. Landau and E. Lifshitz, *Fluid Mechanics: V. 6* (Elsevier Science, 2013).
- [4] R. A. Broglia, A. Molinari, and T. Regge, On the hydrodynamics of Fermi superfluids, *Annals of Physics* **109**, 349 (1977).
- [5] D. Kobayakov and C. J. Pethick, Dynamics of the inner crust of neutron stars: Hydrodynamics, elasticity, and collective modes, *Phys. Rev. C* **87**, 055803 (2013).
- [6] P. D. Fleming and C. Cohen, Hydrodynamics of solids, *Phys. Rev. B* **13**, 500 (1976).
- [7] B. I. Halperin and P. C. Hohenberg, Hydrodynamic Theory of Spin Waves, *Phys. Rev.* **188**, 898 (1969).
- [8] L. Landau, Theory of the Superfluidity of Helium II, *Phys. Rev.* **60**, 356 (1941).
- [9] C. J. Pethick and H. Smith, *Bose-Einstein Condensation in Dilute Gases*, 2nd ed. (Cambridge University Press, 2008).
- [10] A. Griffin, T. Nikuni, and E. Zaremba, *Bose-Condensed Gases at Finite Temperatures* (Cambridge University Press, 2009).
- [11] G. De Rosi and S. Stringari, Collective oscillations of a trapped quantum gas in low dimensions, *Phys. Rev. A* **92**, 053617 (2015).
- [12] L. Pitaevskii and S. Stringari, *Bose-Einstein Condensation and Superfluidity*, International Series of Monographs on Physics (Oxford University Press, Oxford, 2016).
- [13] H. B. Thacker, Exact integrability in quantum field theory and statistical systems, *Rev. Mod. Phys.* **53**, 253 (1981).
- [14] B. Sutherland, *Beautiful Models: 70 years of exactly solved quantum many-body problems* (World Scientific, Singapore, 2004).
- [15] M. Rigol, V. Dunjko, V. Yurovsky, and M. Olshanii, Relaxation in a Completely Integrable Many-Body Quantum System: An Ab Initio Study of the Dynamics of the Highly Excited States of 1D Lattice Hard-Core Bosons, *Phys. Rev. Lett.* **98**, 050405 (2007).
- [16] M. Rigol, V. Dunjko, and M. Olshanii, Thermalization and its mechanism for generic isolated quantum systems, *Nature* **452**, 854 (2008).
- [17] M. A. Cazalilla and M. Rigol, Focus on Dynamics and Thermalization in Isolated Quantum Many-Body Systems, *New Journal of Physics* **12**, 055006 (2010).
- [18] A. Polkovnikov, K. Sengupta, A. Silva, and M. Vengalattore, Colloquium: Nonequilibrium dynamics of closed interacting quantum systems, *Rev. Mod. Phys.* **83**, 863 (2011).
- [19] J. Eisert, M. Friesdorf, and C. Gogolin, Quantum many-body systems out of equilibrium, *Nature Physics* **11**, 124 (2015).
- [20] C. Gogolin and J. Eisert, Equilibration, thermalisation, and the emergence of statistical mechanics in closed quantum systems, *Reports on Progress in Physics* **79**, 056001 (2016).
- [21] E. H. Lieb, Exact Analysis of an Interacting Bose Gas. II. The Excitation Spectrum, *Phys. Rev.* **130**, 1616 (1963).
- [22] C. Menotti and S. Stringari, Collective oscillations of a one-dimensional trapped Bose-Einstein gas, *Phys. Rev. A* **66**, 043610 (2002).
- [23] G. De Rosi, G. E. Astrakharchik, and S. Stringari, Thermodynamic behavior of a one-dimensional Bose gas at low temperature, *Phys. Rev. A* **96**, 013613 (2017).
- [24] N. D. Mermin and H. Wagner, Absence of Ferromagnetism or Antiferromagnetism in One- or Two-Dimensional Isotropic Heisenberg Models, *Phys. Rev. Lett.* **17**, 1133 (1966).
- [25] P. C. Hohenberg, Existence of Long-Range Order in One and Two Dimensions, *Phys. Rev.* **158**, 383 (1967).
- [26] L. D. Landau and E. M. Lifshitz, *Statistical Physics: Vol. 5* (Elsevier Science, 2013).
- [27] A. Minguzzi and M. P. Tosi, Collective excitations in confined Fermi gases, *Physica B: Condensed Matter* **300**, 27 (2001).
- [28] A. Griffin, W.-C. Wu, and S. Stringari, Hydrodynamic Modes in a Trapped Bose Gas above the Bose-Einstein Transition, *Phys. Rev. Lett.* **78**, 1838 (1997).
- [29] M. K. Tey, L. A. Sidorenkov, E. R. S. Guajardo, R. Grimm, M. J. H. Ku, M. W. Zwierlein, Y.-H. Hou, L. Pitaevskii, and S. Stringari, Collective Modes in a Unitary Fermi Gas across the Superfluid Phase Transition, *Phys. Rev. Lett.* **110**, 055303 (2013).
- [30] H. Hu, G. Xianlong, and X.-J. Liu, Collective modes of a one-dimensional trapped atomic Bose gas at finite temperatures, *Phys. Rev. A* **90**, 013622 (2014).
- [31] G. De Rosi and S. Stringari, Hydrodynamic versus collisionless dynamics of a one-dimensional harmonically trapped Bose gas, *Phys. Rev. A* **94**, 063605 (2016).

- [32] A. Sinatra, C. Lobo, and Y. Castin, Classical-Field Method for Time Dependent Bose-Einstein Condensed Gases, *Phys. Rev. Lett.* **87**, 210404 (2001).
- [33] H. Moritz, T. Stöferle, M. Köhl, and T. Esslinger, Exciting Collective Oscillations in a Trapped 1D Gas, *Phys. Rev. Lett.* **91**, 250402 (2003).
- [34] E. Haller, M. Gustavsson, M. J. Mark, J. G. Danzl, R. Hart, G. Pupillo, and H.-C. Nägerl, Realization of an Excited, Strongly Correlated Quantum Gas Phase, *Science* **325**, 1224 (2009).
- [35] R. Schmitz, S. Krönke, L. Cao, and P. Schmelcher, Quantum breathing dynamics of ultracold bosons in one-dimensional harmonic traps: Unraveling the pathway from few- to many-body systems, *Phys. Rev. A* **88**, 043601 (2013).
- [36] B. Fang, G. Carleo, A. Johnson, and I. Bouchoule, Quench-Induced Breathing Mode of One-Dimensional Bose Gases, *Phys. Rev. Lett.* **113**, 035301 (2014).
- [37] X.-L. Chen, Y. Li, and H. Hu, Collective modes of a harmonically trapped one-dimensional Bose gas: The effects of finite particle number and nonzero temperature, *Phys. Rev. A* **91**, 063631 (2015).
- [38] A. I. Gudyma, G. E. Astrakharchik, and M. B. Zvonarev, Reentrant behavior of the breathing-mode-oscillation frequency in a one-dimensional Bose gas, *Phys. Rev. A* **92**, 021601(R) (2015).
- [39] S. Choi, V. Dunjko, Z. D. Zhang, and M. Olshanii, Monopole Excitations of a Harmonically Trapped One-Dimensional Bose Gas from the Ideal Gas to the Tonks-Girardeau Regime, *Phys. Rev. Lett.* **115**, 115302 (2015).
- [40] I. Bouchoule, S. S. Szigeti, M. J. Davis, and K. V. Kheruntsyan, Finite-temperature hydrodynamics for one-dimensional Bose gases: Breathing-mode oscillations as a case study, *Phys. Rev. A* **94**, 051602 (2016).
- [41] F. A. Bayocboc and K. V. Kheruntsyan, Frequency beating and damping of breathing oscillations of a harmonically trapped one-dimensional quasicondensate, *Comptes Rendus. Physique* **24**, 15 (2023).
- [42] B. Laburthe Tolra, K. M. O'Hara, J. H. Huckans, W. D. Phillips, S. L. Rolston, and J. V. Porto, Observation of Reduced Three-Body Recombination in a Correlated 1D Degenerate Bose Gas, *Phys. Rev. Lett.* **92**, 190401 (2004).
- [43] T. Kinoshita, T. Wenger, and D. S. Weiss, Observation of a One-Dimensional Tonks-Girardeau Gas, *Science* **305**, 1125 (2004).
- [44] I. Bouchoule, N. J. van Druten, and C. I. Westbrook, Atom Chips and One-Dimensional Bose Gases, in *Atom Chips* (John Wiley & Sons, Ltd, 2011) Chap. 11, pp. 331–363.
- [45] F. Salces-Carcoba, C. J. Billington, A. Putra, Y. Yue, S. Sugawa, and I. B. Spielman, Equations of state from individual one-dimensional Bose gases, *New Journal of Physics* **20**, 113032 (2018).
- [46] O. A. Castro-Alvaredo, B. Doyon, and T. Yoshimura, Emergent Hydrodynamics in Integrable Quantum Systems Out of Equilibrium, *Phys. Rev. X* **6**, 041065 (2016).
- [47] B. Bertini, M. Collura, J. De Nardis, and M. Fagotti, Transport in Out-of-Equilibrium XXZ Chains: Exact Profiles of Charges and Currents, *Phys. Rev. Lett.* **117**, 207201 (2016).
- [48] B. Doyon, J. Dubail, R. Konik, and T. Yoshimura, Large-Scale Description of Interacting One-Dimensional Bose Gases: Generalized Hydrodynamics Supersedes Conventional Hydrodynamics, *Phys. Rev. Lett.* **119**, 195301 (2017).
- [49] B. Doyon and T. Yoshimura, A note on generalized hydrodynamics: inhomogeneous fields and other concepts, *SciPost Phys.* **2**, 014 (2017).
- [50] M. Schemmer, I. Bouchoule, B. Doyon, and J. Dubail, Generalized Hydrodynamics on an Atom Chip, *Phys. Rev. Lett.* **122**, 090601 (2019).
- [51] B. Doyon, Lecture notes on Generalised Hydrodynamics, *SciPost Phys. Lect. Notes*, 18 (2020).
- [52] A. Bastianello, A. De Luca, and R. Vasseur, Hydrodynamics of weak integrability breaking, *Journal of Statistical Mechanics: Theory and Experiment* **2021**, 114003 (2021).
- [53] V. Alba, B. Bertini, M. Fagotti, L. Piroli, and P. Ruggiero, Generalized-hydrodynamic approach to inhomogeneous quenches: correlations, entanglement and quantum effects, *Journal of Statistical Mechanics: Theory and Experiment* **2021**, 114004 (2021).
- [54] N. Malvania, Y. Zhang, Y. Le, J. Dubail, M. Rigol, and D. S. Weiss, Generalized hydrodynamics in strongly interacting 1D Bose gases, *Science* **373**, 1129 (2021).
- [55] M. L. Kerr and K. V. Kheruntsyan, The theory of generalised hydrodynamics for the one-dimensional Bose gas, *AAPPS Bull.* **33**, 25 (2023).
- [56] R. S. Watson, S. A. Simmons, and K. V. Kheruntsyan, Benchmarks of generalized hydrodynamics for one-dimensional Bose gases, *Phys. Rev. Res.* **5**, L022024 (2023).
- [57] K. V. Kheruntsyan, D. M. Gangardt, P. D. Drummond, and G. V. Shlyapnikov, Finite-temperature correlations and density profiles of an inhomogeneous interacting one-dimensional Bose gas, *Phys. Rev. A* **71**, 053615 (2005).
- [58] G. De Rosi, R. Rota, G. E. Astrakharchik, and J. Boronat, Hole-induced anomaly in the thermodynamic behavior of a one-dimensional Bose gas, *SciPost Phys.* **13**, 035 (2022).
- [59] G. De Rosi, G. E. Astrakharchik, M. Olshanii, and J. Boronat, Thermal fading of the $1/k^4$ tail of the momentum distribution induced by the hole anomaly, *Phys. Rev. A* **109**, L031302 (2024).
- [60] N. P. Raju, E. Gmelin, and R. K. Kremer, Magnetic-susceptibility and specific-heat studies of spin-glass-like ordering in the pyrochlore compounds $R_2\text{Mo}_2\text{O}_7$ ($R=\text{Y}$, Sm , or Gd), *Phys. Rev. B* **46**, 5405 (1992).
- [61] M. J. H. Ku, A. T. Sommer, L. W. Cheuk, and M. W. Zwierlein, Revealing the Superfluid Lambda Transition in the Universal Thermodynamics of a Unitary Fermi Gas, *Science* **335**, 563 (2012).
- [62] A. Tari, *The Specific Heat Of Matter At Low Temperatures* (World Scientific Publishing Company, 2003).
- [63] C. He, H. Zheng, J. F. Mitchell, M. L. Foo, R. J. Cava, and C. Leighton, Low temperature Schottky anomalies in the specific heat of LaCoO_3 : Defect-stabilized finite spin states, *Applied Physics Letters* **94**, 102514 (2009).
- [64] Z. Z. Yan, Y. Ni, C. Robens, and M. W. Zwierlein, Bose polarons near quantum criticality, *Science* **368**, 190 (2020).
- [65] D. S. Petrov, G. V. Shlyapnikov, and J. T. M. Walraven, Regimes of Quantum Degeneracy in Trapped 1D Gases, *Phys. Rev. Lett.* **85**, 3745 (2000).

- [66] M. Olshanii, Atomic Scattering in the Presence of an External Confinement and a Gas of Impenetrable Bosons, *Phys. Rev. Lett.* **81**, 938 (1998).
- [67] E. H. Lieb and W. Liniger, Exact Analysis of an Interacting Bose Gas. I. The General Solution and the Ground State, *Phys. Rev.* **130**, 1605 (1963).
- [68] H. Bethe, Zur Theorie der Metalle. I. Eigenwerte und Eigenfunktionen der linearen Atomkette, *Zeitschrift für Physik* **71**, 205 (1931).
- [69] M. Takahashi, *Thermodynamics of One-Dimensional Solvable Models* (Cambridge University Press, 1999).
- [70] C. N. Yang and C. P. Yang, Thermodynamics of a One-Dimensional System of Bosons with Repulsive Delta-Function Interaction, *Journal of Mathematical Physics* **10**, 1115 (1969).
- [71] C. P. Yang, One-Dimensional System of Bosons with Repulsive δ -Function Interactions at a Finite Temperature T , *Phys. Rev. A* **2**, 154 (1970).
- [72] K. V. Kheruntsyan, D. M. Gangardt, P. D. Drummond, and G. V. Shlyapnikov, Pair Correlations in a Finite-Temperature 1D Bose Gas, *Phys. Rev. Lett.* **91**, 040403 (2003).
- [73] M. L. Kerr, G. De Rosi, and K. V. Kheruntsyan, Analytic thermodynamic properties of the Lieb-Liniger gas, *SciPost Phys. Core* **7**, 047 (2024).
- [74] G. De Rosi, P. Massignan, M. Lewenstein, and G. E. Astrakharchik, Beyond-Luttinger-liquid thermodynamics of a one-dimensional Bose gas with repulsive contact interactions, *Phys. Rev. Research* **1**, 033083 (2019).
- [75] G. De Rosi, R. Rota, G. E. Astrakharchik, and J. Boronat, Correlation properties of a one-dimensional repulsive Bose gas at finite temperature, *New J. Phys.* **25**, 043002 (2023).
- [76] Y. Castin, Simple theoretical tools for low dimension Bose gases, *J. Phys. IV France* **116**, 89 (2004).
- [77] M. Girardeau, Relationship between Systems of Impenetrable Bosons and Fermions in One Dimension, *Journal of Mathematical Physics* **1**, 516 (1960).
- [78] G. De Rosi, Collective oscillations of a trapped atomic gas in low dimensions and thermodynamics of one-dimensional Bose gas (PhD Thesis, Università degli Studi di Trento, 2017).
- [79] F. S. Møller and J. Schmiedmayer, Introducing iFluid: a numerical framework for solving hydrodynamical equations in integrable models, *SciPost Phys.* **8**, 041 (2020).
- [80] G. E. Astrakharchik, J. Boronat, J. Casulleras, and S. Giorgini, Beyond the Tonks-Girardeau Gas: Strongly Correlated Regime in Quasi-One-Dimensional Bose Gases, *Phys. Rev. Lett.* **95**, 190407 (2005).
- [81] A. S. Arkhipov, G. E. Astrakharchik, A. V. Belikov, and Y. E. Lozovik, Ground-state properties of a one-dimensional system of dipoles, *Journal of Experimental and Theoretical Physics Letters* **82**, 39 (2005).
- [82] M. D. Girardeau and G. E. Astrakharchik, Super-Tonks-Girardeau State in an Attractive One-Dimensional Dipolar Gas, *Phys. Rev. Lett.* **109**, 235305 (2012).
- [83] O. N. Osychenko, G. E. Astrakharchik, Y. Lutsyshyn, Y. E. Lozovik, and J. Boronat, Phase diagram of Rydberg atoms with repulsive van der Waals interaction, *Phys. Rev. A* **84**, 063621 (2011).
- [84] G. E. Astrakharchik and J. Boronat, Luttinger-liquid behavior of one-dimensional ^3He , *Phys. Rev. B* **90**, 235439 (2014).
- [85] G. Bertaina, M. Motta, M. Rossi, E. Vitali, and D. E. Galli, One-Dimensional Liquid ^4He : Dynamical Properties beyond Luttinger-Liquid Theory, *Phys. Rev. Lett.* **116**, 135302 (2016).
- [86] A. Del Maestro, N. Nichols, T. Prisk, G. Warren, and P. E. Sokol, Experimental realization of one dimensional helium, *Nature Comm.* **13**, 3168 (2022).
- [87] P. Cheiney, C. R. Cabrera, J. Sanz, B. Naylor, L. Tanzi, and L. Tarruell, Bright Soliton to Quantum Droplet Transition in a Mixture of Bose-Einstein Condensates, *Phys. Rev. Lett.* **120**, 135301 (2018).
- [88] G. De Rosi, G. E. Astrakharchik, and P. Massignan, Thermal instability, evaporation, and thermodynamics of one-dimensional liquids in weakly interacting Bose-Bose mixtures, *Phys. Rev. A* **103**, 043316 (2021).
- [89] Z.-X. Ye, A. Canali, C.-K. Wong, M. Kreyer, E. Kirilov, and R. Grimm, Dipole-mode spectrum and hydrodynamic crossover in a resonantly interacting two-species fermion mixture, *Phys. Rev. Res.* **7**, 023259 (2025).
- [90] H. Hiyane, S. Watabe, and T. Nikuni, Collective excitations of a Bose-condensed gas: Fate of second sound in the crossover regime between hydrodynamic and collisionless regimes, *Phys. Rev. A* **109**, 033302 (2024).
- [91] P. Haensel, Collective excitations of nuclear matter, *Z. Physik A* **277**, 65 (1976).
- [92] G. De Rosi, Superfluidity in neutron star matter (MSc Thesis, Sapienza, Università di Roma, 2013).
- [93] O. Benhar and G. De Rosi, Superfluid Gap in Neutron Matter from a Microscopic Effective Interaction, *J Low Temp Phys* **189**, 250 (2017).
- [94] T. Kinoshita, T. Wenger, and D. S. Weiss, Local Pair Correlations in One-Dimensional Bose Gases, *Phys. Rev. Lett.* **95**, 190406 (2005).
- [95] S. Hofferberth, I. Lesanovsky, B. Fischer, T. Schumm, and J. Schmiedmayer, Non-equilibrium coherence dynamics in one-dimensional Bose gases, *Nature* **449**, 324 (2007).
- [96] P. Krüger, S. Hofferberth, I. E. Mazets, I. Lesanovsky, and J. Schmiedmayer, Weakly Interacting Bose Gas in the One-Dimensional Limit, *Phys. Rev. Lett.* **105**, 265302 (2010).
- [97] J. Armijo, T. Jacqmin, K. V. Kheruntsyan, and I. Bouchoule, Probing Three-Body Correlations in a Quantum Gas Using the Measurement of the Third Moment of Density Fluctuations, *Phys. Rev. Lett.* **105**, 230402 (2010).
- [98] M. Gring, M. Kuhnert, T. Langen, T. Kitagawa, B. Rauer, M. Schreitl, I. Mazets, D. A. Smith, E. Demler, and J. Schmiedmayer, Relaxation and Prethermalization in an Isolated Quantum System, *Science* **337**, 1318 (2012).
- [99] R. Shah, T. J. Barrett, A. Colcelli, F. Oručević, A. Trombettoni, and P. Krüger, Probing the Degree of Coherence through the Full 1D to 3D Crossover, *Phys. Rev. Lett.* **130**, 123401 (2023).
- [100] C. Chin, R. Grimm, P. Julienne, and E. Tiesinga, Feshbach resonances in ultracold gases, *Rev. Mod. Phys.* **82**, 1225 (2010).
- [101] F. Meinert, M. Panfil, M. J. Mark, K. Lauber, J.-S. Caux, and H.-C. Nägerl, Probing the Excitations of a Lieb-Liniger Gas from Weak to Strong Coupling, *Phys. Rev. Lett.* **115**, 085301 (2015).
- [102] A. H. van Amerongen, J. J. P. van Es, P. Wicke, K. V. Kheruntsyan, and N. J. van Druten, Yang-Yang Ther-

- modynamics on an Atom Chip, [Phys. Rev. Lett. **100**, 090402 \(2008\)](#).
- [103] T. Jacqmin, J. Armijo, T. Berrada, K. V. Kheruntsyan, and I. Bouchoule, Sub-Poissonian Fluctuations in a 1D Bose Gas: From the Quantum Quasicondensate to the Strongly Interacting Regime, [Phys. Rev. Lett. **106**, 230405 \(2011\)](#).
- [104] F. Møller, T. Schweigler, M. Tajik, J. a. Sabino, F. Cataldini, S.-C. Ji, and J. Schmiedmayer, Thermometry of one-dimensional Bose gases with neural networks, [Phys. Rev. A **104**, 043305 \(2021\)](#).

End Matter

Appendix A: High- T collisionless regime—At sufficiently high temperatures T , any harmonically trapped gas approaches the ideal classical limit, as the confinement causes a rapid decay in the density profile, which is described by the Maxwell-Boltzmann Gaussian.

For the sake of generality, consider a classical gas of N particles in a three-dimensional (3D) isotropic harmonic trap with frequency ω_{ho} . The corresponding Maxwell-Boltzmann density profile is given by $n_{3\text{D}}(r) = \frac{N}{\pi^{3/2} R_T^3} e^{-r^2/R_T^2}$, where $r = \sqrt{x^2 + y^2 + z^2}$ is the scalar radial coordinate and $R_T = \sqrt{2k_B T / (m\omega_{\text{ho}}^2)}$ is the thermal radius [12]. The collision rate in such a gas is given by $\Gamma = n_{3\text{D}}(r) \sigma v_T$ and depends on the s -wave scattering cross-section $\sigma = 8\pi a^2$ (where a is the 3D s -wave scattering length) and the thermal velocity $v_T \sim \sqrt{T}$. At high T , collisions become rare as the collision rate Γ decreases with temperature according to $\Gamma \sim \sigma v_T / R_T^3 \sim \sigma / T$ [78]. Consequently, a harmonically trapped (i.e., nonuniform) gas necessarily enters the collisionless regime, as $\Gamma \rightarrow 0$ with $T \rightarrow \infty$. In contrast to this, in a uniform system, where the density of the gas $n_{3\text{D}}$ remains constant in r at any T , collisions become more frequent as Γ increases with temperature through its dependence on v_T , which is unchanged.

Appendix B: Parameter values—For most of the datasets (a)–(e) in Fig. 1, our simulations are performed using realistic experimental parameters [33, 34, 36, 42–44, 50, 94–99], with temperatures in the range $T \simeq 60 \div 1000$ nK, total number of atoms $N \gtrsim 80$, and axial and transverse (radial) trap frequencies of $\omega_x/2\pi \simeq 1 \div 10$ Hz and $\omega_\perp/2\pi \simeq 400 \div 2 \times 10^4$ Hz, respectively. To access some of the more extreme physical regimes, however, we had to push the values of these parameters beyond what is currently achievable in experiments. We recall that entering the 1D regime requires $\omega_x \ll \omega_\perp$, along with that both the central chemical potential μ_0 and the thermal energy $k_B T$ satisfy $\{\mu_0, k_B T\} \ll \hbar\omega_\perp$ [96, 99].

We consider ^{87}Rb atoms (with mass $m \simeq 1.443 \times 10^{-25}$ kg) for definiteness, for which the 3D s -wave scattering length is $a \simeq 5.3$ nm. The value of a can be tuned via magnetic Fano-Feshbach resonances [100, 101], which in turn changes the 1D interaction strength $g_{1\text{D}} \simeq 2\hbar\omega_\perp a$ away from confinement-induced resonances [34, 66]. Alternatively, $g_{1\text{D}}$ can be tuned by varying ω_\perp [43, 66, 94]. We note, however, that close to a confinement-induced resonance, where $a \rightarrow a_\perp/C$, one must use the exact expression $g_{1\text{D}} = 2\hbar^2 a / [ma_\perp^2 (1 - Ca/a_\perp)]$, where $a_\perp = \sqrt{\hbar/(m\omega_\perp)}$ is the transverse harmonic oscillator length and $C \simeq 1.0326$ [12, 66].

Temperature can be measured both below and above the hole-induced anomaly threshold T_A in single 1D tubes, using techniques such as time-of-flight, Bose gas

Table II. Values of the dimensionless temperature \mathcal{T} , Eq. (2), the dimensionless 1D scattering length $\tilde{a}_{1\text{D}}$, Eq. (3), the 3D s -wave scattering length a (in meters m), and the dimensionless perturbation strength $\tilde{\lambda} \ll 1$, Eq. (4), for each dataset (a)–(e), corresponding to blue points in Figs. 1 and 3, and to panels (a)–(e) in Fig. 2. All parameter values are chosen such that they satisfy the 1D condition $\{\mu_0, k_B T, \hbar\omega_x\} \ll \hbar\omega_\perp$.

Dataset	\mathcal{T}	$\tilde{a}_{1\text{D}}$	a [m]	$\tilde{\lambda}$
(a)	1.1×10^{-4}	10^{-3}	2.65×10^{-8}	3×10^{-5}
(b)	0.11	1.43×10^{-2}	2.65×10^{-8}	5×10^{-4}
(c)	1.08	3.22×10^{-2}	2.65×10^{-8}	10^{-3}
(d)	6.5×10^2	3.23	5.3×10^{-9}	2×10^{-4}
(e)	1.1×10^4	3.23	5.3×10^{-11}	3.5×10^{-3}

focusing, ideal Bose gas fits to the wings of the *in-situ* density profiles, or measurements of *in-situ* density fluctuations [45, 97, 102, 103]. More recently, advances in thermometry have been achieved using neural networks, trained to extract temperature from a single absorption image taken after time-of-flight expansion [104].

The parameters employed in our simulations of DC oscillations in Fig. 2 for the datasets (a)–(e) are shown in Table II. Here, the temperature \mathcal{T} is defined in Eq. (2). The dimensionless 1D scattering length is given by:

$$\tilde{a}_{1\text{D}} = -a_{1\text{D}}/a_x, \quad (3)$$

where $a_{1\text{D}} = -2\hbar^2/(mg_{1\text{D}}) < 0$ is the 1D scattering length [66] and $a_x = \sqrt{\hbar/(m\omega_x)}$ is the axial harmonic oscillator length. The dimensionless perturbation strength is defined as:

$$\tilde{\lambda} = \lambda a_x^3 / (\hbar\omega_x). \quad (4)$$

As mentioned in the main text, for fixed values of the interaction strength γ_0 and temperature \mathcal{T} , Eq. (2), a third parameter must be specified to fully and uniquely characterize a harmonically trapped 1D Bose gas. This can either be the frequency of the axial confinement ω_x , which fixes the total number of atoms N at a given central density n_0 (or γ_0), or, alternatively, N itself, in which case we treat ω_x as an adjustable input parameter.

In Fig. 3 we report the values of N as a function of γ_0 that we used for each of the datasets (a)–(e) at their respective fixed \mathcal{T} and $\tilde{a}_{1\text{D}}$ as in Table II. By keeping \mathcal{T} constant, we fix the value of $g_{1\text{D}}$ which—together with the condition of constant $\tilde{a}_{1\text{D}}$ —allows us to determine ω_x . For each dataset (a)–(e) in Table II, we also keep fixed both a , which defines ω_\perp via $g_{1\text{D}} = 2\hbar\omega_\perp a$, and the perturbation strength $\tilde{\lambda}$, which is required to excite the dipole-compressional modes.

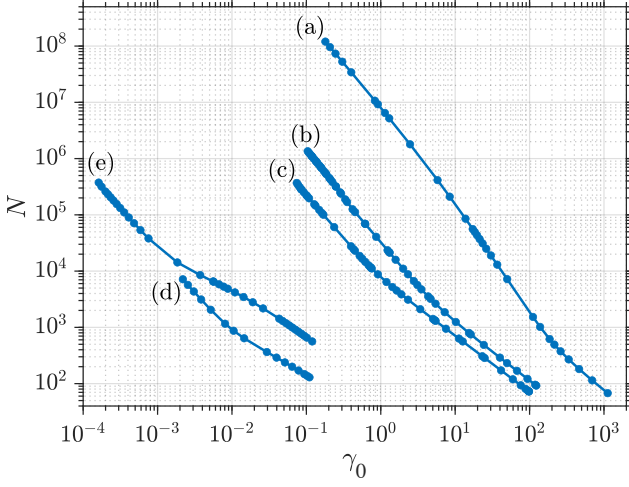


Figure 3. Total atom number N of a harmonically confined 1D Bose gas vs. the interaction strength γ_0 , Eq. (2), defined at the trap centre. Each dataset (a)–(e) (see also Fig. 1) is shown for a fixed value of both temperature \mathcal{T} , Eq. (2), and the 1D scattering length \tilde{a}_{1D} , Eq. (3), as in Table II.

Appendix C: Excitation of DC modes — Collective oscillations are generated by a perturbation $H_{\text{pert}} = -\lambda F(x)\theta(t)$ to the Hamiltonian (1) with a small strength parameter λ . Here, $F(x) = \sum_{i=1}^N f(x_i)$ is the static excitation operator and $\theta(t)$ is the Heaviside function of time t . H_{pert} is implemented as a sudden quench of the external trapping potential $V(x) \rightarrow V(x) - \lambda f(x)$ at $t = 0$ leading to a density perturbation $n(x, t)$.

To excite the dipole compression modes, we choose $f(x)$ as $f_{\text{DC}}(x) = x^3/3 - x\langle x^2 \rangle$, where $\langle x^2 \rangle = \int dx x^2 n(x)/N$ is the average evaluated using the equilibrium density $n(x)$ prior to the quench [78]. The subtraction of the second term in $f_{\text{DC}}(x)$ prevents the excitation of the center-of-mass (dipole) mode [31] whose frequency is ω_x .

Appendix D: Skewness and its Fourier Transform —

To characterize the DC oscillations in the perturbed density $n(x, t)$, we employ the skewness as our probe, which describes the asymmetry of the atomic distribution in the gas cloud following the quench. It is defined as the standardized (i.e., normalized by the standard deviation) third moment of the distribution of atom positions x :

$$\text{Skew}(t) = \frac{\langle (x - \langle x \rangle_t)^3 \rangle_t}{\sigma_x^3(t)}, \quad (5)$$

where $\sigma_x(t) = \sqrt{\langle x^2 \rangle_t - \langle x \rangle_t^2}$ is the standard deviation, and the averages $\langle \cdot \rangle_t$ are evaluated with the instantaneous density $n(x, t)$, which is computed using the gen-

eralized hydrodynamics method. We note that the third moment of the atom number distribution in a 1D Bose gas was measured in Ref. [97], suggesting that skewness could likewise be accessed in state-of-the-art experiments probing the same system.

We analyse $\text{Skew}(t)$ in frequency space by performing its discrete Fourier transform (FT), which is real for the norm $\| \cdot \|$, and is given by:

$$\text{FT}[\text{Skew}](\omega_k) = \left\| \sum_{j=0}^{\mathcal{N}_t-1} f(t_j) e^{-i\omega_k t_j} \right\|, \quad k = 0, \dots, \mathcal{N}_t - 1, \quad (6)$$

where $f(t) = \text{Skew}(t) - \langle \text{Skew}(t) \rangle_t$ and we subtract the average background signal $\langle \text{Skew}(t) \rangle_t$ from the actual skewness $\text{Skew}(t)$ to eliminate the peak at zero frequency. We define the discrete time as $t_j = j\Delta t$, where Δt is the time step, and the total evolution time as $t_{\text{tot}} = \mathcal{N}_t \Delta t$, with \mathcal{N}_t the number of time steps. The discrete DC frequency components are given by $\omega_k = 2\pi k/t_{\text{tot}}$.

Figure 4 (1) shows a GHD calculation of the skewness $\text{Skew}(t)$, Eq. (5), as a function of time. Figure 4 (2) presents the corresponding Fourier transform, Eq. (6), where the positions of the peaks indicate the two dominant frequency components, ω_1 and ω_2 . Their relative excitation strengths are quantified by K_1 and $K_2 = 1 - K_1$, where $K_1 = h_1^2/(h_1^2 + h_2^2)$ and $h_{1,2}$ are the peak heights [41]. In this case, the DC oscillations exhibit a beating between $\omega_1 \simeq 1\omega_x$ and $\omega_2 \simeq 3\omega_x$, consistent with predictions for the collisionless regime [31], although with unequal strengths ($K_1 > K_2$), unlike in Table I.

By repeating this analysis across datasets (a)–(e) in Fig. 1, we extract the DC oscillation frequencies and their excitation strengths throughout the various regimes of the 1D Bose gas, as shown in Fig. 2 of the main text.

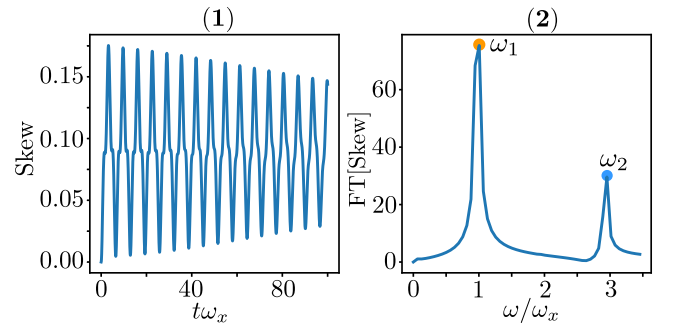


Figure 4. (1): Example of the skewness, Eq. (5), vs. the dimensionless time $t\omega_x$, calculated for dataset (c) (see Table II) at $\gamma_0 = 5.035$, corresponding to $N = 1412$ in Fig. 3. (2): Fourier transform of the skewness in (1), $\text{FT}[\text{Skew}]$, Eq. (6), vs. frequency ω/ω_x . The yellow and blue markers at the two peaks correspond to the DC oscillation frequencies ω_1 and ω_2 .